

Electron-Transfer Kinetics in Sulfonated Aluminum Phthalocyanines/Cytochrome *c* Complexes

César A. T. Laia,^{*,†} Sílvia M. B. Costa,[†] David Phillips,[‡] and Andrew Beeby[§]

Centro de Química-Estrutural, Complexo 1, Instituto Superior Técnico, 1049-001 LISBOA, Portugal, Department of Chemistry, Imperial College, Exhibition Road, London SW7 2AY, U.K., and Chemistry Department, University of Durham, South Road, Durham DH1 3LE, U.K.

Received: September 8, 2003; In Final Form: February 4, 2004

Sulfonated aluminum phthalocyanines interact with cytochrome *c* forming complexes in aqueous solutions. The binding of these dyes was probed using fluorescence techniques (steady-state spectroscopy and time-correlated single photon counting), which enable the calculation of the equilibrium binding constants. The fluorescence of the complex is relatively low ($\phi = 0.07$) due to an electron-transfer process from the phthalocyanine singlet-excited state to the cytochrome *c*. The binding constant determines the amount of fluorescence and is quite high for the tetrasulfonated aluminum phthalocyanine ($3.3 \times 10^5 \text{ M}^{-1}$) while those for the disulfonated and monosulfonated aluminum phthalocyanines are one order of magnitude smaller. The fluorescence decays suggest more than one location for the dye adsorbed in the protein, which is affected by electrostatic interactions, leading to nonexponential decays.

Introduction

Electron-transfer reactions between small molecules and macromolecules such as proteins can provide valuable information on the mechanisms of metabolic processes such as photosynthesis and respiration, and also lead to the development of new devices for applications on the storage of solar energy and molecular switches.^{1–6} One key protein in such studies is cytochrome *c* (Cyt *c*), essentially due to the fact that it is water soluble, has a relatively low molecular weight, and is quite stable.^{4,7} During the past few years, electron-transfer between selected donors and Cyt *c* was studied extensively. The heme group in the Cyt *c* has Fe(III) in the center of the ring, which changes to Fe(II) due to a direct electron-transfer reaction.^{4,7–27}

More recently, it was shown that some water-soluble organic molecules such as tetrasulfonated porphyrins can complex with Cyt *c* with high affinity through noncovalent interactions.^{28–33} Such molecules can interact with the lysine and arginine residues present on the surface of the Cyt *c* allowing the docking between this protein (which acts as an electron carrier in the cell) and Cyt *c* oxidase. Such interaction can disrupt the bond between both proteins and can shed some light on the mechanisms of protein–ligand complexation.

The fluorescence of porphyrins complexed with Cyt *c* is strongly quenched due to electron-transfer from the singlet-excited state of solutes to the heme group of Cyt *c*.^{16,23,30,32} It is thus relatively easy to follow the binding by fluorescence spectroscopy and time-resolved emission measurements. However, details of this electron-transfer are still not well understood. Indeed, the complex fluorescence decay of uroporphyrin was found to be not single exponential,^{16,23} which led to several possible explanations: either it is caused by a distribution of

electron-transfer rate constants^{16,23,34–40} or by a dynamic conformational rearrangement during the singlet excited-state lifetime (so-called “gated electron-transfer”).^{7,11,16,22–24,41–44}

Phthalocyanines have a structure similar to porphyrins.^{45,46} Sulfonated phthalocyanines have a negative electric charge which allows its solubilization in water.⁴⁶ Previous work with tetrasulfonated aluminum phthalocyanine (AlPcS₄) showed that this dye can form charge-transfer complexes with methyl viologen.⁴⁷ In the present work, it is shown that AlPcS₄ also binds to Cyt *c* with a great affinity. Due to the electron-transfer process between the singlet excited of AlPcS₄ and Cyt *c*, the fluorescence is quenched when the complex is formed. Mono-sulfonated and disulfonated aluminum phthalocyanines were also studied (AlPcS₁ and AlPcS₂, respectively), and it is shown that the net charge is a key aspect in the binding of these molecules to Cyt *c*, leading to smaller affinities of the dyes toward the protein. The fluorescence decays are affected by the details of the solute/protein interaction; AlPcS₄ exhibits faster decays due to the stronger binding.

Experimental Section

AlPcS₄ was purchased from Porphyrin Products (99% purity) and used as received. AlPcS₁ and AlPcS₂ were synthesized according to Ambroz et al.⁴⁸ Cyt *c* from the horse heart was purchased from Aldrich (97% purity) and used without further purification. Solvents used were bidistilled water and spectroscopic ethanol and glycerol from Aldrich.

Absorption spectra were recorded at room temperature with a JASCO V-560 UV–vis absorption spectrophotometer. Steady-state emission measurements were recorded with a Perkin-Elmer LS 50B spectrofluorimeter with the sample holder thermostated at 22 °C. The instrumental response at each wavelength was corrected by means of a curve provided with the instrument. Due to the Cyt *c* strong absorption at the excitation wavelength where the emission spectra were measured, in these experiments it is not possible to use [Cyt *c*] above 100 μM , in order to have an absorbance around 0.1 at the excitation wavelength.

* Corresponding author. Fax: +351218419274. Phone: +351218419274. E-mail: cesar.laia@popsrv.ist.utl.pt.

[†] Instituto Superior Técnico.

[‡] Imperial College.

[§] University of Durham.

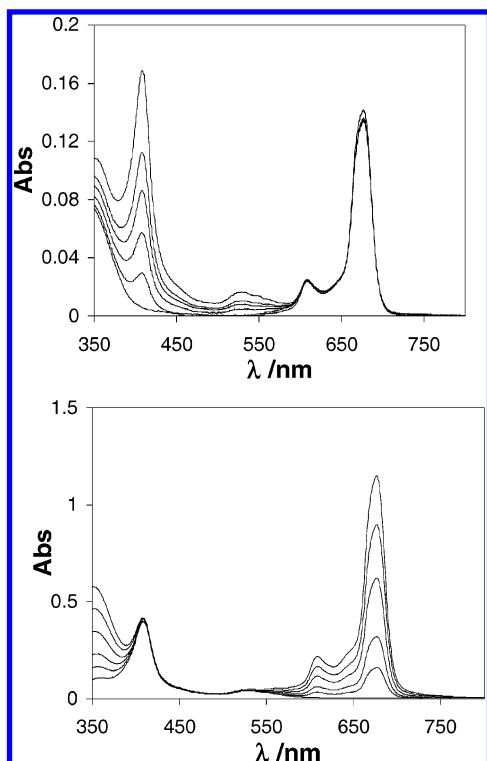


Figure 1. Absorption spectra of AlPcS₄/Cyt *c* mixtures in water. (A) [AlPcS₄] = 1 μM and [Cyt *c*] = 0–1.7 μM. (B) [AlPcS₄] = 0–8 μM and [Cyt *c*] = 4 μM.

Time correlated single photon counting was used to obtain the fluorescence decays.⁴⁹ The excitation source consisted of a pulsed 635 nm diode laser (IBH NanoLED model-02) providing output pulses of <200 ps at a repetition rate of 1 MHz. The fluorescence emission was collected at 90° to the excitation source, and the emission wavelength was selected using a monochromator (Jobin Yvon Triax 190). The fluorescence was detected using a cooled, red sensitive photomultiplier tube (IBH Model TBX-04) linked to a time-to-amplitude converter (Ortec 567) and multichannel analyzer (E.G.&G. Trump Card and Maestro for Windows v.5.10). The instrument response function (IRF) of the apparatus was measured using a dilute suspension of Ludox in water as a scattering medium giving an IRF with a duration of 450 ps full width at half-maximum (fwhm). The time per channel was 25 ps giving a full range of 25 ns over the 1024 point data set. All fluorescence decays were recorded to a minimum of 10 000 counts in the peak channel of the pulse height analyzer. The data were transferred to a computer and analyzed by using a program developed previously,⁵⁰ based on iterative deconvolution method and nonlinear least-squares fitting. The quality of the fits was judged from statistical parameters such as the χ^2 (below 1.2), Durbin–Watson (DW) parameter (above 1.8), and the homogeneous distribution of the residuals.

Unless it is stated otherwise, the phthalocyanines' concentration was always 1 μM.

Results and Data Analysis

Absorption Spectra. Phthalocyanines generally present a small solvatochromism. The small shifts of the monomer absorption spectra can be correlated with $f(n^2) = (n^2 - 1)/(2 \times n^2 + 1)$, indicating changes of the solute polarizability.⁵¹ That behavior is understandable due to the fact that these molecules do not have a significant dipole moment; therefore, the contribution from liquid orientational polarization is negligible.

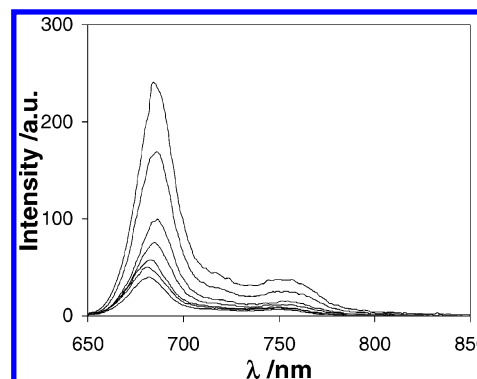


Figure 2. Fluorescence emission spectra of AlPcS₄ in water for [Cyt *c*] = 0–130 μM.

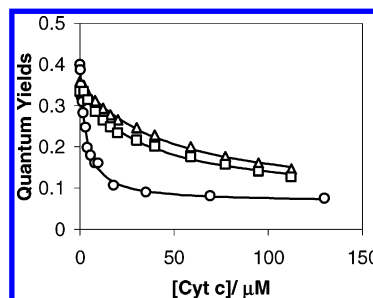
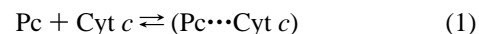


Figure 3. Fluorescence quantum yield of AlPcS₁ (□), AlPcS₂ (Δ), and AlPcS₄ (○) in water vs [Cyt *c*].

The absorption spectra of AlPcS₄ in cytochrome solutions reflect this behavior (see Figure 1), where a significant solvatochromic shift upon the increase of protein concentration is not observed. The absorption spectra correspond to what would be expected from the sum of the AlPcS₄ and Cyt *c* spectra alone, whether [AlPcS₄] or [Cyt *c*] is changed. No charge-transfer absorption band from the AlPcS₄ to the heme group is observed. Although the results for AlPcS₂ and AlPcS₁ are not shown, the spectra obtained are very similar.

Emission Spectra. The effect of the Cyt *c* contribution to the sulfonated phthalocyanines photophysics is evident when the emission spectra are measured (see Figure 2). As the concentration of Cyt *c* increases, the phthalocyanine fluorescence intensity decreases, even for concentrations as low as 1 μM. This indicates a strong ground-state association between the dye (Pc) and the protein, which should be a consequence of a very high binding constant K_b .³²



$$K_b = \frac{[(\text{Pc})(\text{Cyt } c)]}{[\text{Pc}(\text{aq})][\text{Cyt } c]} \quad (2)$$

It is usually assumed that emission from the complex is negligible. However as one can see in Figure 3, the fluorescence quantum yield of AlPcS₄ reaches a plateau at high concentrations of Cyt *c*, while that of AlPcS₂ and AlPcS₁ also decreases but the quenching is less effective. This is an indication that the complex indeed has an appreciable emission. A different approach was thus used, in which the emission of the complex is also considered.^{32,52} Thus

$$\phi = \frac{\phi_0 + \phi_{\text{complex}} K_b [\text{Cyt } c]}{1 + K_b [\text{Cyt } c]} \quad (3)$$

where ϕ_0 is the Pc fluorescence quantum yield in water and ϕ_{complex} is the complex fluorescence quantum yield. This

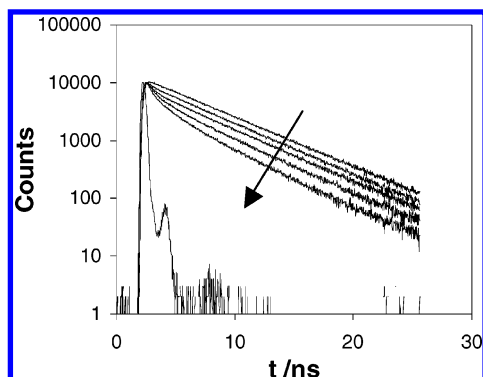


Figure 4. AlPcS₄ fluorescence decays in water for [Cyt *c*] = 0–396 μM.

TABLE 1: Binding Constants to Cyt *c* and Electric Charge of the Phthalocyanines in Distilled Water

compound	charge	ϕ_0	ϕ_{complex}	K_b/M^{-1}
AlPcS ₁	−1	0.40	0.07	29 500
AlPcS ₂	−2	0.36	0.06	20 950
AlPcS ₄	−4	0.34	0.07	330 000

TABLE 2: Results of the Data Analysis of the AlPcS₄ Fluorescence Decays in Water with Model 1^a

[Cyt <i>c</i>]/μM	a_1	τ_1/ns	a_2	τ_2/ns	a_3	τ_3/ns	χ^2	DW
0	1.000	5.027					1.042	1.858
2	0.972	4.982			0.028	0.767	0.995	2.100
4	0.966	4.925			0.034	0.498	1.018	1.944
8	0.944	4.865			0.056	0.468	0.993	1.714
20	0.610	4.818	0.178	0.987	0.211	0.217	1.037	1.988
40	0.451	4.710	0.253	1.033	0.297	0.199	1.153	1.836
60	0.392	4.669	0.252	1.325	0.356	0.249	1.056	1.811
79	0.364	4.634	0.235	1.364	0.400	0.310	1.089	1.899
119	0.355	4.581	0.299	1.331	0.345	0.244	1.223	1.798
158	0.340	4.513	0.274	1.515	0.387	0.327	1.016	2.055
396	0.271	4.351	0.320	1.377	0.409	0.247	1.072	1.752
Global Analysis (τ_2 and τ_3 Common)								
0	1.000	5.027					1.042	1.858
2	0.933	4.995	0.036	1.472	0.032	0.315	0.994	2.104
4	0.899	4.944	0.034	1.472	0.067	0.315	1.015	1.953
8	0.820	4.900	0.052	1.472	0.128	0.315	0.949	1.797
20	0.574	4.857	0.122	1.472	0.304	0.315	1.012	2.028
40	0.426	4.777	0.181	1.472	0.393	0.315	1.108	1.914
60	0.392	4.687	0.224	1.472	0.384	0.315	1.080	1.774
79	0.384	4.665	0.239	1.472	0.376	0.315	1.095	1.892
119	0.315	4.613	0.257	1.472	0.428	0.315	1.143	1.931
158	0.293	4.501	0.261	1.472	0.445	0.315	1.017	2.053
396	0.198	4.373	0.241	1.472	0.562	0.315	0.999	1.880

^a See text for explanation.

equation is valid as long as the absorption at the excitation wavelength does not change with [Cyt *c*], which is true in our experiments ($\lambda_{\text{ex}} = 640$ nm). A very reasonable fit is obtained with eq 3 for the three systems, and the results are shown in Table 1.

Fluorescence Decays. (a) *AlPcS₄/Cyt *c* in Water.* The AlPcS₄ fluorescence decays were obtained at $\lambda_{\text{em}} = 690$ nm, changing the Cyt *c* concentration. These results show monoexponential decays for AlPcS₄ in water, as expected, but as the protein concentration increases the decays become clearly nonexponential (see Figure 4 and Table 2). Visually, it is possible to distinguish an initial nonexponential component for the solutions with the highest Cyt *c* concentration, followed by an exponential tail with roughly the same lifetime of the AlPcS₄ alone.

To analyze these decays we can distinguish several models for the AlPcS₄ binding to the Cyt *c*. The simplest would be to postulate a very specific interaction with a protein site. Since it is assumed that only one complex structure is formed, the

TABLE 3: Results of the Data Analysis of the AlPcS₄ Fluorescence Decays in Water with a Sum of an Exponential with Model 2

[Cyt <i>c</i>]/μM	a_1	τ_1/ns	a_2	τ_2/ns	α	χ^2	DW
0	1.000	5.027				1.042	1.858
2	0.892	5.009	0.108	0.540	0.614	0.983	2.105
4	0.760	4.955	0.240	0.233	0.577	0.981	1.949
8	0.576	4.912	0.424	0.129	0.462	0.934	1.809
20	0.385	4.845	0.615	0.189	0.519	0.992	2.056
40	0.245	4.782	0.755	0.177	0.471	1.068	1.963
60	0.197	4.624	0.803	0.173	0.418	0.986	1.927
79	0.218	4.682	0.782	0.248	0.477	1.027	1.962
119	0.164	4.504	0.836	0.212	0.433	1.055	1.997
158	0.175	4.468	0.825	0.275	0.467	1.002	2.039
396	0.124	4.144	0.876	0.217	0.439	0.951	1.952
Global Analysis (τ_2 and α Common)							
0	0.953	5.039	0.047	0.173	0.420	0.966	1.907
2	0.828	4.998	0.172	0.173	0.420	0.988	2.094
4	0.698	4.976	0.302	0.173	0.420	0.995	1.919
8	0.569	4.942	0.431	0.173	0.420	1.016	1.668
20	0.336	4.899	0.664	0.173	0.420	1.119	1.850
40	0.216	4.798	0.784	0.173	0.420	1.184	1.789
60	0.193	4.641	0.807	0.173	0.420	1.039	1.828
79	0.187	4.588	0.813	0.173	0.420	1.053	1.920
119	0.161	4.476	0.839	0.173	0.420	1.089	1.926
158	0.158	4.340	0.842	0.173	0.420	1.074	1.892
396	0.121	4.084	0.879	0.173	0.420	0.985	1.875

distance between the phthalocyanines and the heme group⁴¹ would be the same and the decays would be biexponential.

However, the biexponential model was found to be not adequate for our systems. It describes well the decays for low concentrations of Cyt *c*, but for higher concentrations the quality of the fits deteriorates, giving rise to unacceptable χ^2 and inhomogeneous distribution of the residuals. To achieve a satisfactory fit, at least a sum of 3 exponentials is needed, which could imply another binding site in the Cyt *c* to keep the model consistent, where a_1 , a_2 , and a_3 are the preexponential factors and τ_1 , τ_2 , and τ_3 are the decay times (model 1):

$$I(t) = a_1 \exp\left(-\frac{t}{\tau_1}\right) + a_2 \exp\left(-\frac{t}{\tau_2}\right) + a_3 \exp\left(-\frac{t}{\tau_3}\right) \quad (4)$$

A global fit with eq 4 keeping τ_2 and τ_3 constant for all [Cyt *c*] leads to good fits of the fluorescence decays, which means that within the experimental error the decay components of the complex are independent of the protein concentration (see Table 2). In an alternative interpretation, the AlPcS₄ may be located in many places around the protein and a distribution of donor–acceptor distances should be taken into account,^{34–40} using this simple equation³⁸ (model 2):

$$I(t) = a_1 \exp\left(-\frac{t}{\tau_{\text{water}}}\right) + a_2 \exp\left[-\left(\frac{t}{\tau_{\text{comp}}}\right)^\alpha\right] \quad (5)$$

which shows a sum of an exponential with a stretched exponential, where τ_{comp} is the stretched time constant of the fluorescence decay and α is an empirical exponent indicating the degree of deviation from linearity. Equation 5 is easy to use, but it is only an empirical expression.

The decays from this work were also analyzed with model 2 (see Table 3). An individual analysis of the fluorescence decays shows τ_2 (equivalent to τ_{comp} on model 2) and α reasonably invariant within the range of [Cyt *c*] studied and the inherent covariance of the parameters of the data analysis. The results for low [Cyt *c*] are the ones that present a smaller degree of confidence due to the low pre-exponential factor of the complex decay and are also those deviating more from the general trend.

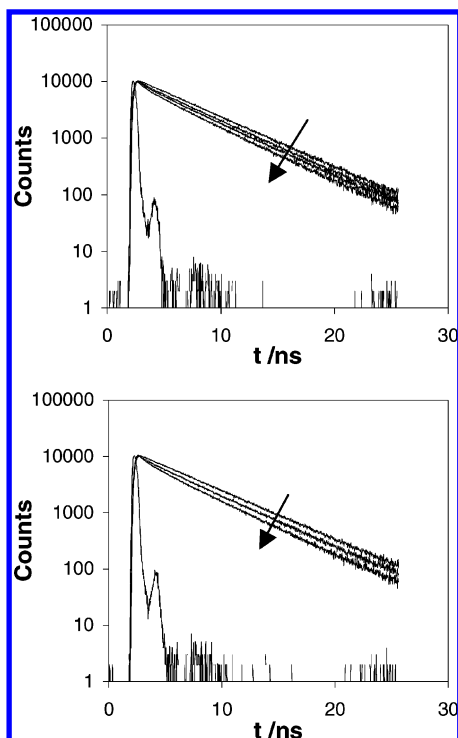


Figure 5. Fluorescence decays in water for [Cyt *c*] = 0–396 μM : (A) AlPcS₁, (B) AlPcS₂.

Interestingly, however, τ_1 (which corresponds to τ_{water}) changes with the [Cyt *c*] in such a way that cannot be dismissed as covariance of the parameters. This indicates a significant diffusion process in which the free AlPcS₄ forms a complex with the Cyt *c* within its singlet excited-state lifetime.

(b) *AlPcS₂ and AlPcS₁/Cyt *c* in Water.* The influence of the molecular charge on the complex formation and electron-transfer to Cyt *c* was studied following the fluorescence decay of the phthalocyanine derivatives AlPcS₁ and AlPcS₂. These molecules are very similar to AlPcS₄ and are still water-soluble,⁴⁶ but the overall charge is smaller, decreasing the importance of electrostatic interactions. As expected, this has a very important impact on the fluorescence decays (Figure 5). The component of the complex decay for both dyes has lower pre-exponential factors for the same [Cyt *c*] when compared with AlPcS₄ (see Tables 4 and 5). The complex component is again nonexponential, but it can be only seen for high concentrations of Cyt *c*, due to its low preexponential factor.

(c) *Electron-Transfer Rate Constants.* In both global analyses, a good fit is only obtained if the decay component of the unbound species is not fixed. This means that within our time-scale the dye can diffuse toward the protein and form a complex. In such circumstances, the diffusion rate constant should be of the order of $10^{10} \text{ M}^{-1} \text{ s}^{-1}$, and the complex can dissociate or not within our time scale. The kinetic scheme for the interaction of an excited-state phthalocyanine Pc and Cyt *c* has to consider an extra step for the interaction between solute and protein. Scheme 1 describes the situation in which there is a specific binding driven by electrostatic interactions and an unspecific binding where hydrophobic interactions play an important role. This scheme gives rise to triexponential decays, which is equivalent to model 1 that fits our experimental results successfully.

According to the fluorescence steady-state results, the binding constant for molecules with negative charge is higher than 10^4 M^{-1} (see Table 1); therefore, for $k_{\text{diff}} \approx 10^{10} \text{ M}^{-1} \text{ s}^{-1}$ the k_{diss} should be lower than 10^6 s^{-1} , and thus, it may be considered

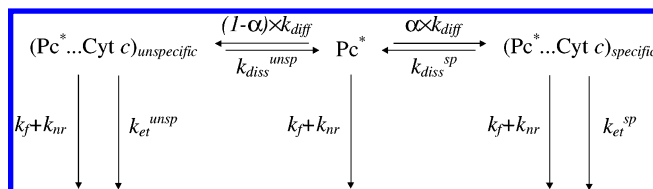
TABLE 4: Results of the Data Analysis of the AlPcS₁ and AlPcS₂ Fluorescence Decays in Water with Model 1

[Cyt <i>c</i>]/ μM	a_1	τ_1/ns	a_2	τ_2/ns	a_3	τ_3/ns	χ^2	DW
AlPcS ₁								
0	1.000	4.863					1.086	1.879
4	0.962	4.915	0.044	2.122	−0.006	0.436	0.996	1.994
8	0.973	4.879	0.022	2.122	0.005	0.436	1.032	2.061
20	0.936	4.899	0.056	2.122	0.009	0.436	0.907	1.944
40	0.906	4.854	0.070	2.122	0.024	0.436	1.007	2.024
59	0.860	4.850	0.094	2.122	0.046	0.436	1.022	1.793
79	0.757	4.827	0.110	2.122	0.133	0.436	1.005	2.029
119	0.809	4.802	0.128	2.122	0.063	0.436	1.002	1.990
158	0.776	4.769	0.136	2.122	0.088	0.436	1.026	2.069
396	0.634	4.670	0.179	2.122	0.187	0.436	1.045	1.878
AlPcS ₂								
0	1.000	4.960					1.068	1.836
3	0.981	4.981	0.023	1.932	−0.003	0.419	1.039	1.839
6	0.977	4.988	0.029	1.932	−0.006	0.419	0.903	2.012
12	0.970	4.978	0.032	1.932	−0.002	0.419	0.928	2.046
29	0.934	4.958	0.051	1.932	0.015	0.419	0.959	2.086
59	0.888	4.913	0.085	1.932	0.026	0.419	1.020	1.851
88	0.868	4.868	0.088	1.932	0.045	0.419	1.034	2.066
118	0.852	4.846	0.110	1.932	0.039	0.419	1.088	2.005
412	0.678	4.650	0.184	1.932	0.138	0.419	0.963	2.038

TABLE 5: Results of the Data Analysis of the AlPcS₁ and AlPcS₂ Fluorescence Decays in Water with a Sum of an Exponential with Model 2

[Cyt <i>c</i>]/ μM	a_1	τ_1/ns	a_2	τ_2/ns	α	χ^2	DW
AlPcS ₁							
0	0.969	4.882	0.031	0.541	0.499	1.045	1.921
4	0.940	4.886	0.060	0.541	0.499	1.010	1.921
8	0.940	4.866	0.060	0.541	0.499	1.021	2.049
20	0.873	4.860	0.127	0.541	0.499	0.907	1.904
40	0.786	4.811	0.214	0.541	0.499	0.972	2.014
59	0.716	4.791	0.284	0.541	0.499	0.999	1.795
79	0.684	4.761	0.316	0.541	0.499	0.990	2.018
119	0.636	4.721	0.364	0.541	0.499	1.010	2.009
158	0.597	4.680	0.403	0.541	0.499	0.992	2.056
396	0.482	4.521	0.518	0.541	0.499	1.029	1.903
AlPcS ₂							
0	0.997	4.973	0.003	0.625	0.526	1.063	1.843
3	0.976	4.968	0.024	0.625	0.526	1.012	1.807
6	0.980	4.963	0.020	0.625	0.526	0.905	1.953
12	0.948	4.963	0.052	0.625	0.526	0.945	2.003
29	0.856	4.939	0.144	0.625	0.526	0.936	2.078
59	0.777	4.876	0.223	0.625	0.526	1.038	1.831
88	0.711	4.847	0.289	0.625	0.526	1.038	2.053
118	0.677	4.812	0.323	0.625	0.526	1.074	1.990
412	0.483	4.564	0.517	0.625	0.526	0.909	2.084

SCHEME 1



negligible during the singlet excited-state lifetime ($5 \times 10^{-9} \text{ s}$). This simplifies Scheme 1, which therefore is given by the differential equation^{53,54}

$$-\frac{d}{dt} \begin{bmatrix} \text{Pc}^* \\ \text{Pc}_{\text{sp}}^* \\ \text{Pc}_{\text{unsp}}^* \end{bmatrix} = \begin{bmatrix} X + k_{\text{diff}}[\text{Cyt } c] & 0 & 0 \\ \alpha k_{\text{diff}}[\text{Cyt } c] & X + k_{\text{et}}^{\text{sp}} & 0 \\ (1 - \alpha)k_{\text{diff}}[\text{Cyt } c] & 0 & X + k_{\text{et}}^{\text{unsp}} \end{bmatrix} \times \begin{bmatrix} \text{Pc}^* \\ \text{Pc}_{\text{sp}}^* \\ \text{Pc}_{\text{unsp}}^* \end{bmatrix} \quad (6)$$

TABLE 6: Kinetic Constants Obtained from the Decay Analysis of Scheme 1 for Model 1 and (b) the Average Decay Times of Model 2

	model 1			av decay times of model 2		
	$k_{\text{diff}}/\text{M}^{-1} \text{ s}^{-1}$	$k_{\text{et}}^{\text{sp}}/\text{s}^{-1}$	$k_{\text{et}}^{\text{unsp}}/\text{s}^{-1}$	$k_{\text{diff}}/\text{M}^{-1} \text{ s}^{-1}$	$\langle \tau_{\text{comp}} \rangle / \text{s}$	$\langle k_{\text{et}} \rangle / \text{s}^{-1}$
AlPcS ₁	2.5×10^{10}	2.1×10^9	2.7×10^8	4.2×10^{10}	1.085	7.2×10^8
AlPcS ₂	3.5×10^{10}	2.2×10^9	3.2×10^8	4.4×10^{10}	1.143	6.7×10^8
AlPcS ₄		3.0×10^9	4.8×10^8		0.504	1.8×10^9

where X is given by

$$X = k_f + k_{\text{nr}} \quad (7)$$

For reasons of simplicity, X is considered to be the same in the 3 species Pc^* , Pc_{sp}^* , and $\text{Pc}_{\text{unsp}}^*$. This is reasonable since it was shown that phthalocyanine photophysics is not greatly affected by the environment. The fluorescence lifetime is around 5–6 ns, which gives $X \approx 2 \times 10^8 \text{ s}^{-1}$. The solutions for the decay lifetimes are obtained from the following third-order equation:

$$\begin{vmatrix} X + k_{\text{diff}}[\text{Cyt } c] - \lambda & 0 & 0 \\ \alpha k_{\text{diff}}[\text{Cyt } c] & X + k_{\text{et}}^{\text{sp}} - \lambda & 0 \\ (1 - \alpha)k_{\text{diff}}[\text{Cyt } c] & 0 & X + k_{\text{et}}^{\text{unsp}} - \lambda \end{vmatrix} = 0 \quad (8)$$

The equation can be easily solved, giving

$$\lambda_1 = X + k_{\text{diff}}[\text{Cyt } c] \quad (9)$$

$$\lambda_2 = X + k_{\text{et}}^{\text{sp}} \quad (10)$$

$$\lambda_3 = X + k_{\text{et}}^{\text{unsp}} \quad (11)$$

Therefore, in this model each recovered decay component is assigned to the decays of each species. The decay component assigned to the free phthalocyanine when plotted versus $[\text{Cyt } c]$ should give a linear Stern–Volmer relationship according to this scheme.

For model 2, the kinetic scheme is of course more complicated. It would be an extension of Scheme 1, which assumed a large number of sites on the protein surface with which the molecule can interact. Therefore, $\lambda_2, \lambda_3, \dots, \lambda_n$ are within the distribution of decay lifetimes given by the stretched exponential,^{55,56} and λ_1 is still given by eq 9. The time dependence of k_{et} would be included only on the stretched exponential decay of the complex, and therefore, its nonexponential character would include the dynamic conformational fluctuations occurring during the lifetime of the singlet excited state. The average fluorescence lifetime of the complex can be calculated with eq 12⁵⁵

$$\langle \tau_{\text{comp}} \rangle = \frac{1}{\alpha} \Gamma\left(\frac{1}{\alpha}\right) \tau_{\text{comp}} \quad (12)$$

where $\Gamma(x)$ is the gamma function. This enables the calculation of an average value for the electron-transfer rate constant, eq 13

$$\langle k_{\text{et}} \rangle = \frac{1}{\langle \tau_{\text{comp}} \rangle} - \frac{1}{\tau_0} \quad (13)$$

where τ_0 is the fluorescence lifetime without the quenching process.

The results calculated for k_{et} and k_{diff} for the three dyes are shown in Table 6.

Discussion

Absorption and Emission Spectroscopy. The absorption spectra of the phthalocyanines remain almost unchanged when Cyt c is added. Previously, it was shown the AlPcS₄ exhibits charge-transfer interactions with an electron acceptor methyl viologen,⁴⁷ affecting both absorption and emission spectra, but with Cyt c the absorption of both acceptor and donor remain unchanged.

However, the fluorescence intensity decreases with $[\text{Cyt } c]$ showing the existence of an electron-transfer reaction between the singlet excited state and Cyt c . An energy transfer fluorescence quenching is ruled out because the energy of the singlet excited state could only be transferred to the charge-transfer absorption heme band which appears at 695 nm with an extinction coefficient less than $800 \text{ M}^{-1} \text{ cm}^{-1}$. According to Forster theory,⁵⁷ the rate constant of energy transfer is less than 10^6 s^{-1} , which is too slow to be detected in fluorescence experiments. Thus, the phthalocyanine singlet excited states are mainly quenched by the electron-transfer process, with a unimolecular rate constant around 10^9 s^{-1} .

The AlPcS₄ has a strong affinity for Cyt c , as one can judge by the high K_b (around 10^5 M^{-1}). This result was obtained in distilled water, and it is of the same order of magnitude as previously obtained for tetrasulfonated porphyrins. Such high affinity is an indication that the molecule is located in the specific region of the Cyt c , with the appropriate positively charged domains on the surface of the protein that come from the presence of lysine residues, where cytochrome c oxidase also binds. Such location allows a short distance between the solute and the heme group, which enhances the electron-transfer rate constant.

The AlPcS₂ and AlPcS₁ have values of K_b that are one order of magnitude lower. The chemical structure of these dyes is very similar; however, the electric charge is lower reducing the electrostatic interactions with the Cyt c binding site. Figure 6 compares our results with others published in the literature.^{16,23,32} Those measurements were performed at a low ionic strength solution, and they all compare well. Some variations of more than one order of magnitude, however, highlight the importance of hydrophobic interactions due to the fact that the phthalocyanine and the porphyrin aromatic ring are quite apolar. In fact,

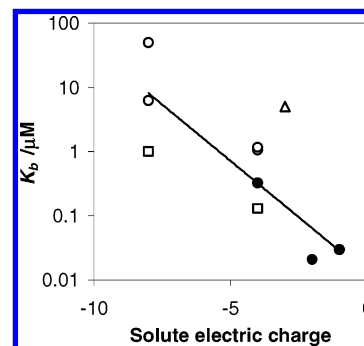


Figure 6. Binding constants of water-soluble porphyrins (data taken from ref 32 for \circ , refs 16 and 23 for \square , and ref 58 for \triangle) and sulfonated phthalocyanines (this work and ref 1).

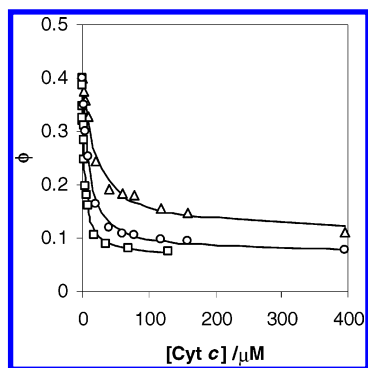


Figure 7. Comparison of AlPcS₄ fluorescence quantum yields obtained from integration of the fluorescence decays vs steady-state results. (□, fluorescence quantum yields; ○, obtained from integration of eq 5; Δ, obtained from integration of eq 4).

those molecules are water insoluble unless the presence of ionic groups in their structure promotes the solubilization of the dyes in water. The higher K_b for AlPcS₁ when compared with AlPcS₂ is a good example of such an effect. Although the electric charge decreases, the solute is more apolar leading to a greater disruption of the solvent hydrogen bond network than in the AlPcS₄ case. Therefore, it is more favorable for the solute to rest nearby apolar sites of the protein than in the bulk water due to entropic reasons. The result obtained by Lahiri et al.⁵⁸ in this context is remarkable, and the high K_b must be attributed to the presence of a long hydrophobic aliphatic chain in the porphyrin (which has -3 charge), that also gives a surfactant-like structure to the molecules, enhancing the interaction with membranes. K_b for the interaction between Cyt *c* and cytochrome *c* oxidase is around $0.10 \mu\text{M}$ at pH = 6 potassium phosphate buffer, ionic strength equal to 50 mM,¹⁹ and around $0.42 \mu\text{M}$ at pH = 7 phosphate buffer, ionic strength equal to 5 mM.³²

Fluorescence Decays. The quenching of the AlPcS₄ fluorescence by Cyt *c* leads to complex fluorescence decays which reflect the presence of the dye in two forms, one is in the bulk water and the other is complexed with protein. While the bulk water form presents a monoexponential decay, the complexed form presents a shorter nonexponential decay that can be easily observed in Figure 4. The decays were analyzed with two different models, which may be explained with different kinetic schemes, reflecting distinct molecular interactions. The analysis with model 1 reflects a system where two distinct locations can be assigned for the interaction between the phthalocyanine and Cyt *c*, while the analysis with model 2 may reflect a much more complex situation with different dye distribution or dynamics.

To check out which of these two models gives the best phenomenological description, we should compare both analyses with the steady-state fluorescence data. The fluorescence intensity at steady-state conditions is given by

$$I = \int_0^\infty I(t) dt \quad (14)$$

The fluorescence quantum yield can be estimated from the fluorescence decays, and compared with the steady-state results. Figure 7 shows such a plot for AlPcS₄. Model 1 leads to estimates of fluorescence quantum yields which are clearly higher than those measured in steady-state conditions. This shows that some components of the fluorescence decays are not taken into account in this analysis, namely in the beginning of the decay. Model 2, however, seems to capture most of such components. That faster component of the stretched exponential is shown in Figure 8.

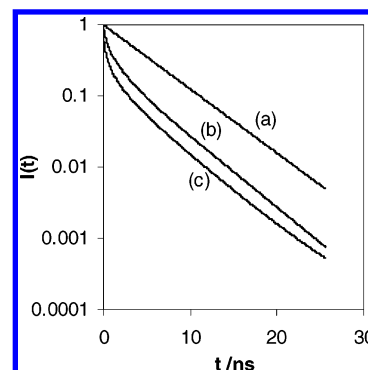


Figure 8. Graphical representations of the AlPcS₄ decays for [Cyt *c*] = $396 \mu\text{M}$ assuming (a) monoexponential decay, (b) triexponential decay, and (c) a sum of an exponential and a stretched exponential decay.

At first sight, it is not easy to explain the existence of many sites for the interaction, because Cyt *c* is not a very large protein. However, it has been shown that water-soluble porphyrins exhibit nonexponential decay when complexed with Cyt *c*, which was attributed to a distribution of distances between the solute and the heme group.^{16,23} The formula used to fit the decays was a Gaussian distribution of lifetimes plus an exponential decay of the unbound porphyrin.²³ In the present work, model 2 also leads to a distribution of decay times, which can be calculated from eq 15^{55,56}

$$e^{-(t/\tau_s)^\alpha} = \int_0^\infty e^{-t/\tau} \rho(\tau) d\tau \quad (15)$$

where $\rho(\tau)$ is the distribution of single exponentials and τ_s has the same meaning as τ_{comp} on eq 6. A solution for $\rho(\tau)$ was found and is given by

$$G[\log(\tau)] = \tau \rho(\tau) = \frac{\tau}{\pi \tau_s} \sum_{n=1}^{\infty} \frac{(-1)^{n+1} \Gamma(n\alpha + 1)}{n!} \left(\frac{\tau}{\tau_s} \right)^{n\alpha - 1} \sin(n\pi\alpha) \quad (16)$$

where $G[\log(\tau)]$ is the distribution of relaxation times of the decay. Equation 16 is quite unstable and difficult to calculate when $\tau > \tau_s$, because it is an alternating series.⁵⁵ A simpler solution is found for $\alpha = 0.5$:

$$G[\log(\tau)] = \frac{1}{2} \left(\frac{\tau}{\tau_s} \right)^{1/2} e^{-\tau/4\tau_s} \quad (17)$$

Therefore, in this case it is easy to calculate the distribution profile. Interestingly enough, the α experimentally obtained is close to 0.5.

The fluorescence decays of AlPcS₄, AlPcS₂, and AlPcS₁ at $396 \mu\text{M}$ were fitted fixing $\alpha = 0.5$. While for eq 17 the results for AlPcS₂ and AlPcS₁ were similar ($\tau_{\text{comp}} = 0.550$ ns), for AlPcS₄ the decay was shorter as expected ($\tau_{\text{comp}} = 0.285$ ns). Figure 9 A shows $G[\log(\tau)]$ for the two cases. The results point out that eq 6 indeed gives an insightful phenomenological description of the complex fluorescence decay. The experimental time resolution of our equipment can reach about 20 ps (10% of the instrumental response full width at the half-maximum, around 200 ps). The difference from a triexponential analysis is striking. While the decay analyzed with model 1 gives rise to a shortest lifetime around 0.3 ns, the distribution of the stretched exponential gives rise to components way below this threshold. For $\tau < 0.1$ ns, there is still an important contribution to the overall complex fluorescence decay.

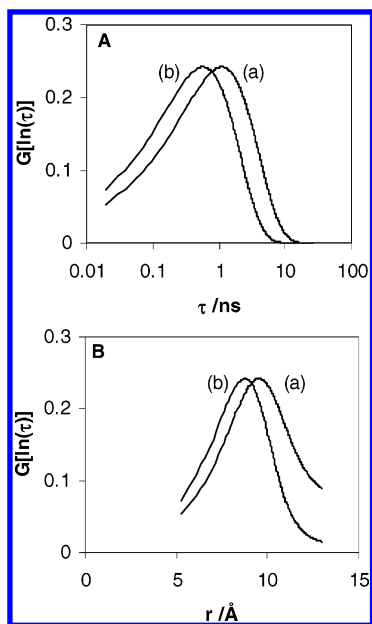


Figure 9. Distribution of relaxation times in (a) Cyt *c*/AlPcS₂ and (b) Cyt *c*/AlPcS₄ systems: (A) versus the relaxation time; (B) versus the edge to edge donor–acceptor distance.

This distribution of relaxation times for the fluorescence complex decay can be converted to electron-transfer rate constant distribution. According to the semiclassical formulation of the Marcus theory,¹ the electron-transfer rate constant is given by eq 18

$$k_{\text{et}} = \sqrt{\frac{4\pi^3}{h^2\lambda k_{\text{B}}T}} H_0^2 \exp(-\beta r) \exp\left(-\frac{(\Delta G^\circ + \lambda)^2}{4\lambda k_{\text{B}}T}\right) \quad (18)$$

where λ is the reorganization energy, h is the Planck constant, k_{B} is the Boltzmann constant, T is the temperature, ΔG° is the reaction driving force, H_0^2 is the electronic coupling for close-contact distance between donor and acceptor, and β is the distance decay constant of the electronic coupling. The electron-transfer reaction kinetics depends on the distance r between the reactants. Therefore, a set of distance distributions leads to a set of possible electron-transfer rates, affecting the overall fluorescence decay.

ΔG° for the electron-transfer from the singlet excited-state phthalocyanines to the Cyt *c* can be calculated and is equal to -0.91 eV. Previous experiments on complexes of organic donors and Cyt *c* have shown that the reorganization energy is around 0.8 eV.^{59,60} Because $\Delta G^\circ \approx -\lambda$, previous experiments in cytochrome *c* showed that the electron-transfer rate constant is approximately given by⁵⁹

$$k_{\text{et}} \approx 10^{13} \exp(-\beta r) \quad (19)$$

when β is around 1 \AA^{-1} . Therefore, a plot of $G[(\log(\tau))]$ as a function of r can be represented (see Figure 9B). It is found that for AlPcS₄ the r at which the electron-transfer process is most likely to occur is 9 \AA , while for AlPcS₁ and AlPcS₂ it is 9.5 \AA . On average, however, $\langle r \rangle$ is 9.8 \AA for AlPcS₄ and 10.5 \AA for AlPcS₁ and AlPcS₂.

This distance is in fact given by

$$r = R - R_0 \quad (20)$$

where R is the distance between the redox sites and R_0 is the close-contact distance. If R_0 is taken to be 3 \AA , then the solutes

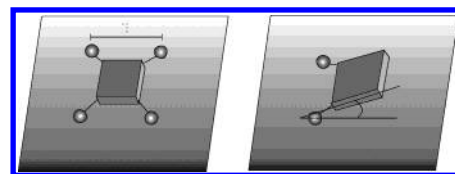


Figure 10. Schematic view of the orientation of the phthalocyanines toward the protein surface.

are approximately 13 \AA away from the iron in the cytochrome *c* heme group. Such short distance is required because the rate obtained in our experiments (higher than 10^8 s^{-1}) is considerably higher than those obtained in cytochrome *c* using other electron donors. In fact, the maximum electron-transfer rate constant reported is around 10^7 s^{-1} ,⁶⁰ which is at least one order of magnitude lower than the rate constant obtained in this work. This indicates that the phthalocyanines are very close to the protein core, and possibly, there is an effect of hydrophobic interactions due to the phthalocyanine aromaticity within the Cyt *c* active site, the site where cytochrome *c* oxidase and other synthetic receptors may dock to the Cyt *c*.

The difference between AlPcS₄ and the other solutes can be explained by assuming different angles for the interaction with the protein surface. Due to the positive electric charge of the binding site, the asymmetry of charge location on AlPcS₂ and AlPcS₁ makes the binding looser at the edges of the solutes with a fewer number of sulfonated groups (see Figure 10). This makes the distance r slightly higher

$$r = R^{\text{min}} + \frac{d}{2} \sin(\theta) - R_0 \quad (21)$$

where R^{min} is R when the solute is horizontally aligned with the protein surface, d is the solute size, and θ is the angle between the solute plane and the protein surface plane. It is likely that $\theta \approx 0^\circ$ for AlPcS₄, due to its symmetric charge distribution and planarity. In such conditions, θ for AlPcS₂ and AlPcS₁ can be estimated at different orientations imposed by angles θ_{A} and θ_{B} :

$$\ln\left(\frac{k_{\text{et}}^{\text{A}}}{k_{\text{et}}^{\text{B}}}\right) = \frac{d}{2} [\sin \theta_{\text{B}} - \sin \theta_{\text{A}}] \quad (22)$$

Using the data of k_{et} on Table 6 (with d equal to 5 \AA and $\theta_{\text{AlPcS}_4} = 0^\circ$), a value of $\theta_{\text{B}} \approx 22^\circ$ is obtained for both AlPcS₂ and AlPcS₁.

Even though the angle θ may affect the coupling between donor and acceptor, it does not account for the large distribution of electron-transfer rate constants obtained, using either model 1 or 2. It is more likely that although the interaction is specific, the nonexponential decay cannot be solely linked to the variation of the angle θ . Dynamical structural rearrangements during the solute excited-state lifetime may change r ,^{11,22,24,42–44,60} so the values obtained for this parameter indicate the distance at which the solute undergoes the electron-transfer with greater probability, not the distance of the solute from the heme group in equilibrium conditions. To study the effect of orientation and dynamical rearrangements, experiments either at low temperatures or high viscosities are needed. However, the electron-transfer process does not depend significantly on temperature in the range $273\text{--}353 \text{ K}$, which means that cryogenic experiments would be required. Measurements in water/sucrose mixtures have been carried out, but no viscosity effect could be detected, which may indicate that dynamical rearrangements do not play a major role.

The binding region of this kind of synthetic receptors has been assigned in a region rich in lysine residues.²⁹ The donor–acceptor distances calculated are in full agreement with such location; thus, especially for AlPcS₄ this is very likely to be the preferred spot. For a more “nonspecific” location (which might play a role specially for AlPcS₁), the more apolar regions on the Cyt *c* surface are the best candidates. However, one should note that the locations probed by this technique are only those in which the electron-transfer is feasible, that is, where $k_{\text{et}} > 10^7 \text{ s}^{-1}$ or $R < 13 \text{ \AA}$. Outside these boundaries, the fluorescence lifetime does not change because the fluorescence process is much faster than the electron-transfer.

The presence of different isomers of AlPcS₂ and AlPcS₄, due to different positions where the sulfonated groups are linked into the aromatic ring, should also be considered. While this has a negligible impact on the dye photophysics in solution,⁴⁶ it still could play a role in the dye adsorption on the surface of the protein. Our results, however, suggest that such effect is negligible in this system as well. In fact the decays for AlPcS₁ also show nonexponential kinetics, which is quite similar to AlPcS₂. AlPcS₄ has a slightly lower α , which indicates a broader distribution, and in fact, this molecule has a greater number of regioisomers; thus, this difference might be explained by this effect. Nevertheless, it is a small effect compared with other sources of nonexponentiality considering the AlPcS₁ results.

Since electrostatic interactions are important in the complex formation, it is expected that the ionic strength will have a major influence on the complex formation. Indeed, preliminary experiments changing the ionic strength were performed, and they showed a strong decrease of K_b . However, no significant changes could be observed in the excited-state complex decay kinetics. Therefore, these preliminary experiments suggest that ionic strength is not important for the electron-transfer dynamics within the complex, although it is important for the binding constant K_b .

Another possibility is that k_{diff} and k_{et} in the Scheme 1 are time-dependent; i.e., there are diffusion transients or relaxations within the excited-state lifetime that give rise to a nonexponential decay.⁶¹ When the quencher concentration is high, the diffusion coefficient D is low (or liquid viscosity high), and the separation radius R is high; then, there is a high probability that some of the quencher molecules are already within the so-called activation volume, at distances close to R . In such cases, the so-called transient diffusion appears because the diffusion rate constant is time-dependent. The presence of such transient would appear at early times of the fluorescence decay below our time resolution (20 ps), and this effect cannot be excluded to explain the fact that eq 5 does not account for all the quenching observed.

Conclusions

The fluorescence of sulfonated aluminum phthalocyanines is greatly reduced in the presence of cytochrome *c* through the formation of 1:1 complexes and a photoinduced electron-transfer. The binding constant is particularly high ($3.3 \times 10^5 \text{ M}$) for the tetrasulfonated molecule due to the favorable electrostatic interactions established with the protein. The fluorescence decays reveal nonexponential components assigned to the complexes. The average unimolecular electron-transfer rate constants are around $1 \times 10^9 \text{ s}^{-1}$, being higher for the tetrasulfonated dye which indicates a tighter complex and a shorter distance between donor and acceptor moieties.

Acknowledgment. This work was supported by CQE IV, Project POCTI/QUI/35398/2000, the Department of Chemistry

of the Imperial College, EPSRC, and the Luso-British Exchange Program from the British Council. C.A.T.L. acknowledges a postdoctoral fellowship, PRAXIS XXI/BPD/22089/99, and the special financial support for his stay in the Imperial College from Fundação Para a Ciência e Tecnologia (FCT). Dr. J. A. B. Ferreira is acknowledged for his valuable help concerning the analysis of the fluorescence decays.

References and Notes

- (1) Marcus, R. A.; Sutin, N. *Biochim. Biophys. Acta* **1985**, *811*, 265–322.
- (2) Frauenfelder, H.; Wolynes, P. G. *Science* **1985**, *229*, 337–345.
- (3) McLendon, G. *Acc. Chem. Res.* **1988**, *21*, 160–167.
- (4) Gray, H. B.; Winkler, J. R. *Annu. Rev. Biochem.* **1996**, *65*, 537–561.
- (5) Frauenfelder, H.; Wolynes, P. G.; Austin, R. H. *Rev. Mod. Phys.* **1999**, *71*, S419–S430.
- (6) Purrelo, R.; Gurrieri, S.; Lauceri, R. *Coord. Chem. Rev.* **1999**, *190–192*, 683–706.
- (7) Nocek, J. M.; Zhou, J. S.; De Forest, S.; Priyadarshy, S.; Beratan, D. N.; Onuchic, J. N.; Hoffman, B. M. *Chem. Rev.* **1996**, *96*, 2459–2489.
- (8) Koppenol, W. H.; Margoliash, E. *J. Biol. Chem.* **1982**, *257*, 4426–4437.
- (9) Roberts, V. A.; Freeman, H. C.; Olson, A. J.; Tainer, J. A.; Getzoff, E. D. *J. Biol. Chem.* **1991**, *266*, 13431–13441.
- (10) Wallace, C. J. A.; Clark-Lewis, I. *J. Biol. Chem.* **1992**, *267*, 3852–3861.
- (11) Zhou, J. S.; Kostic, N. M. *J. Am. Chem. Soc.* **1993**, *115*, 10796–10804.
- (12) Speh, S.; Elias, H. *J. Biol. Chem.* **1994**, *269*, 6370–6375.
- (13) Pascher, T.; Chesick, J. P.; Winkler, J. R.; Gray, H. B. *Science* **1996**, *271*, 1558–1560.
- (14) Kotlyar, A. B.; Borovok, N.; Hazani, M. *Biochemistry* **1997**, *36*, 15823–15827.
- (15) Kotlyar, A. B.; Borovok, N.; Hazani, M. *Biochemistry* **1997**, *36*, 15828–15833.
- (16) Larsen, R. W.; Omdal, D. H.; Jasuja, R.; Niu, S. L.; Jameson, D. M. *J. Phys. Chem. B* **1997**, *101*, 8012–8020.
- (17) Ivkovic-Jensen, M. M.; Kostic, N. M. *Biochemistry* **1997**, *36*, 8135–8144.
- (18) Muegge, I.; Qi, P. X.; Wand, A. J.; Chu, Z. T.; Warshel, A. *J. Phys. Chem. B* **1997**, *101*, 825–836.
- (19) Erman, J. E.; Kresheck, G. C.; Vitello, L. B.; Miller, M. A. *Biochemistry* **1997**, *36*, 4054–4060.
- (20) Tezcan, F. A.; Winkler, J. R.; Gray, H. B. *J. Am. Chem. Soc.* **1998**, *120*, 13383–13388.
- (21) Pettigrew, G. W.; Prazeres, S.; Costa, C.; Palma, N.; Krippahl, L.; Moura, I.; Moura, J. J. G. *J. Biol. Chem.* **1999**, *274*, 11383–11389.
- (22) Mei, H.; Wang, K.; Peffer, N.; Weatherly, G.; Cohen, D. S.; Miller, M.; Pielak, G.; Durham, B.; Millet, F. *Biochemistry* **1999**, *38*, 6846–6854.
- (23) Croney, J. C.; Helms, M. K.; Jameson, D. M.; Larsen, R. W. *J. Phys. Chem. B* **2000**, *104*, 973–977.
- (24) Pletneva, E. V.; Fulton, D. B.; Kohzuma, T.; Kostic, N. M. *J. Am. Chem. Soc.* **2000**, *122*, 1034–1046.
- (25) Jensen, T. J.; Gray, H. B.; Winkler, J. R.; Kuznetsov, A. M.; Ulstrup, J. *J. Phys. Chem. B* **2000**, *104*, 11556–11562.
- (26) Macyk, J.; van Eldik, R. *J. Chem. Soc., Dalton Trans.* **2001**, 2288–2292.
- (27) Pletneva, E. V.; Crnogorac, M. M.; Kostic, N. M. *J. Am. Chem. Soc.* **2002**, *124*, 14342–14354.
- (28) Babine, R. E.; Bender, S. L. *Chem. Rev.* **1997**, *97*, 1359–1472.
- (29) Peczu, M. W.; Hamilton, A. D. *Chem. Rev.* **2000**, *100*, 2479–2494.
- (30) Clark-Ferris, K. K.; Fischer, J. *J. Am. Chem. Soc.* **1985**, *107*, 5007–5008.
- (31) Takashima, H.; Shinkai, S.; Hamachi, I. *Chem. Commun.* **1999**, 2345–2346.
- (32) Jain, R. K.; Hamilton, A. D. *Org. Lett.* **2000**, *2*, 1721–1723.
- (33) Wei, Y.; McLendon, G. L.; Hamilton, A. D.; Case, M. A.; Purring, C. B.; Lin, Q.; Park, H. S.; Lee, C.-S.; Yu, T. *Chem. Commun.* **2001**, 1580–1581.
- (34) Alberty, W. J.; Bartlett, P. N.; Wilde, C. P.; Darwent, J. R. *J. Am. Chem. Soc.* **1985**, *107*, 1854–1858.
- (35) Siebrand, W.; Wildman, T. A. *Acc. Chem. Res.* **1986**, *19*, 238–243.
- (36) Lin, Y.; Dorfman, R. C.; Fayer, M. D. *J. Chem. Phys.* **1989**, *90*, 159–170.
- (37) Gabowska, J.; Hajzner, A.; Chojnowski, A.; Sienicki, K. *J. Chem. Phys.* **1993**, *99*, 1172–1177.

- (38) Levin, P. P.; Costa, S. M. B.; Ferreira, L. F. V. *J. Phys. Chem.* **1995**, *99*, 1267–1275.
- (39) Murata, S.; Tachiya, M. *J. Phys. Chem.* **1996**, *100*, 4064–4070.
- (40) McMahon, B. H.; Müller, J. D.; Wraight, C. A.; Nienhaus, G. U. *Biophys. J.* **1998**, *74*, 2567–2587.
- (41) Hoffman, B. M.; Ratner, M. A. *J. Am. Chem. Soc.* **1987**, *109*, 6237–6243.
- (42) Kurzynski, M.; Palacz, K.; Chelminiak, P. *Proc. Natl. Acad. Sci. U.S.A.* **1998**, *95*, 11685–11690.
- (43) Davidson, V. L. *Acc. Chem. Res.* **2000**, *33*, 87–93.
- (44) Davidson, V. L. *Biochemistry* **2002**, *41*, 14633–14636.
- (45) Fleischer, E. B. *Acc. Chem. Res.* **1970**, *3*, 105–112.
- (46) Phillips, D. *Prog. React. Kinet.* **1997**, *22*, 176–300.
- (47) Laia, C. A. T.; Costa, S. M. B.; Phillips, D.; Parker, A. W. *Photochem. Photobiol. Sci.* **2003**, *2*, 555–562.
- (48) Ambroz, M.; Beeby, A.; MacRobert, A. J.; Simpson, M. S. C.; Svenson, R. K.; Phillips, D. *J. Photochem. Photobiol., B* **1991**, *9*, 87–95.
- (49) FitzGerald, S.; Farren, C.; Stanley, C. F.; Beeby, A.; Bryce, M. R. *Photochem. Photobiol. Sci.* **2002**, *1*, 581–587.
- (50) Ferreira, J. A. B.; Coutinho, P. J. G.; Costa, S. M. B.; Martinho, J. M. G. *Chem. Phys.* **2000**, *262*, 453–465.
- (51) Renge, I. *J. Phys. Chem.* **2000**, *104*, 7452–7463.
- (52) Foley, M. S. C.; Beeby, A.; Parker, A. W.; Bishop, S. M.; Philips, D. *J. Photochem. Photobiol., B* **1997**, *38*, 10–17.
- (53) Berberan-Santos, M. N.; Martinho, J. M. G. *J. Chem. Educ.* **1990**, *67*, 375–379.
- (54) Laia, C. A. T.; Costa, S. M. B. *J. Chem. Soc., Faraday Trans.* **1998**, *94*, 2367–2373.
- (55) Lindsey, C. P.; Patterson, G. D. *J. Chem. Phys.* **1980**, *73*, 3348–3357.
- (56) Svare, I.; Martin, S. W.; Borsa, F. *Phys. Rev. B* **2000**, *61*, 228–233.
- (57) Lakowicz, J. R. *Principles of Fluorescence Spectroscopy*; Plenum Press: New York, 1983.
- (58) Lahiri, J.; Fate, G. D.; Ungashe, S. B.; Groves, J. T. *J. Am. Chem. Soc.* **1996**, *118*, 2347–2358.
- (59) Langen, R.; Chang, I.-Jy; Germanas, J. P.; Richards, J. H.; Winkler, J. R.; Gray, H. B. *Science* **1995**, *268*, 1733–1735.
- (60) Khoshtariya, D. E.; Wei, J.; Liu, H.; Yue, H.; Waldeck, D. H. *J. Am. Chem. Soc.* **2003**, *125*, 7704–7714.
- (61) Sikorski, M.; Krystkowiak, E.; Steer, R. P. *J. Photochem. Photobiol., A* **1998**, *117*, 1–16.